ARTICLE TYPE

Synthesis of Novel Thieno[3,2-*b*]thienobis(silolothiophene) Based Low Bandgap Polymers for Organic Photovoltaics

Bob C. Schroeder,[a] **Raja Shahid Ashraf,***[a] **Stuart Thomas,**[b] **Andrew J. P. White,**[a] **Laure Biniek,**[a] **Christian B. Nielsen,**[a] **Weimin Zhang,**[a] **Zhenggang Huang,**[a] **Pabitra Shakya Tuladhar,**[a] **Scott E. Watkins,**[c]

[5] **Thomas D. Anthopoulos,**[b] **James R. Durrant**[a] **and Iain McCulloch**[a]

Thieno[3,2-*b*]thienobis(silolothiophene), a new electron rich hexacyclic monomer has been synthesized and incorporated
[10] **into three novel donor-acceptor low-bandgap polymers. By carefully choosing the acceptor co-monomer, the energy levels of the polymers could be modulated and high power conversion efficiencies of 5.52% were reached in OPV devices.**

[15] The development of organic photovoltaic cells has received a lot of attention during the last decade and performances of 10% have now been achieved.[1, 2] The design of new semiconducting materials has played a crucial role in this development and recent donor-acceptor polymers have little structural similarity with the

[20] well studied poly(3-hexylthiophene) (**P3HT**).[3] These polymers must be considered as not only photon absorbers in bulk heterojunction (BHJ) solar cells, but also with regard to future commercialization, ambient stability and solution processability, which are key criteria in design. Indacenodithiophene (**IDT**), a

[25] ladder type donor moiety has been successfully introduced into semiconducting polymers, which exhibited excellent hole mobilities in organic field effect transistors (OFET) and good photocurrent efficiencies in organic photovoltaic cells (OPV).[4-7] We have demonstrated that the judicious choice of bridging atom

[30] can not only have an influence on the crystallinity and solubility, but also allows modulating the frontier energy levels.[8] The introduction of silicon as a bridging atom between adjacent aromatic units has several beneficial effects besides increasing the effective conjugation length and reducing the conformational

[35] disorder. The tetravalent silicon offers the possibility to attach solubilising alkyl side chains, which allows tuning the solubility and processability of the polymer. Given the fact that a silicon-carbon bond is slightly longer than a carbon-carbon bond, the anti-bonding lobes located on the butadiene fragments adjacent to

[40] the silicon bridge are separated further from each other, which ultimately should lead to a reduction of the highest occupied molecular orbital (HOMO) energy level.[9] This reduction of the HOMO manifests as an increase in solar cell open circuit voltage and a potential increase in efficiency.

[45] The substitution of the central benzene ring in the **IDT** unit with a less aromatic thieno[3,2-*b*]thiophene has been shown to promote the electron donating character of the monomer.[10] Due to

synthetic limitations, the hexacyclic thieno[3,2-*b*]thiophene based donor units reported so far are substituted with para-alkylated

[50] benzene rings, which can lead to undesirable nanoscale morphologies, causing low fill factors (FF) in OPV devices and limiting performance to 2.5%.[10, 11] Herein we report a high yielding and versatile synthetic route towards a new silicon bridged ladder type donor, thieno[3,2-*b*]thienobis

[55] (silolothiophene) (**Si4T**). The incorporation of silicon as a bridging atom should therefore not only have an effect on the frontier energy levels, but also allow introducing linear alkyl side chains onto the hexacyclic donor moiety.

The synthesis of **Si4T** and the corresponding polymers is

[60] shown in Scheme 1. The α-positions of commercially available 3,6-dibromothieno[3,2-*b*]thiophene (**1**) were iodated and via a selective Negishi coupling between **2** and (3-bromothiophen-2-yl)zinc bromide, the 3,6-dibromo-2,5-bis(3-bromothiophen-2-yl)thieno[3,2-*b*]thiophene (**3**) could be assembled. In order to

[65] improve solubility of **3** and to minimize the possibility of side-reactions during the following synthetic steps, the free α-positions of **3** were lithiated and subsequently quenched with chlorotrimethylsilane to afford compound **4**. The ring-closure was induced by lithiation of all four brominated positions on

[70] compound **4** and by slowly quenching the reaction with dichlorodioctylsilane. Single crystals of **5** were grown from an acetonitrile/diethyl ether mixture, and X-ray studies confirmed both the chemical structure and the planarity of the fused **Si4T** unit, the central $C_{14}Si_4S_4$ unit being coplanar to within ca. 0.03 Å

[75] (Figure 1).

In order to incorporate the new hexacyclic donor unit into low-bandgap polymers via Stille coupling, the trimethylsilane groups

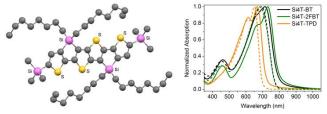**Figure 1.** Single crystal structure of compound **5** (left). Normalized
[80] optical absorption spectra of **Si4T** polymers (right) in dilute chlorobenzene (CB) solution (dashed lines) and as thin films (full lines) spin-cast from CB solution.

Scheme 1. Synthetic route towards the novel **Si4T** monomer and polymers.

were cleaved with *N*-bromosuccinimide before compound **6** was
5 stannylated. All three polymers were synthesized by microwave
assisted Stille polycondensations by reacting one equivalent of
distannylated monomer **7** with one equivalent of the
corresponding dibrominated co-monomer (**A**). All polymers were
purified by a series of Soxhlet extractions and were recovered as
10 dark fibrous solids with high molecular weights (Table 1).
Thermal gravimetric analysis (TGA) (Figure S5 in the ESI)
confirmed that all **Si4T** polymers are stable above 420°C.
Differential scanning calorimetry (DSC) did not show significant
thermal transitions for any of the polymers (Figure S6 in the ESI).
15   Density functional theoretical (DFT) studies predict the lowest
lying HOMO energy level for the **Si4T-TPD** polymer and a
homogenous distribution of both frontier energy levels along the
polymer backbone (Figure S8 in the ESI). The energy levels for
Si4T-BT and **Si4T-2FBT** are calculated to be the same, with the
20 HOMO in both cases delocalized over the polymer backbone, but
the LUMO mainly localized on the **BT** and **2FBT** units
respectively (Figures S7 and S9 in the ESI).
    Polymer **Si4T-BT** was obtained by co-polymerizing monomer
7 with benzo[*c*] [1,2,5]thiadiazole (**BT**). The polymer has a very
25 broad thin film absorption in the visible range extending from
400 up to 800 nm with two absorption bands, one with a
maximum around 450 nm from the π-π* transition and a much
stronger intramolecular charge transfer (ICT) absorption band
with a maximum at 714 nm (Figure 1). The ionisation potential of
30 the polymers were measured as thin films by photoelectron
spectroscopy in air (PESA). The measured HOMO energy level
of **Si4T-BT** was around -5.0 eV. Replacement of the **BT** unit
with thieno[3,4-*c*]pyrrole-4,6-dione (**TPD**) led to an 0.3 eV lower
HOMO energy level in the **Si4T-TPD** polymer (Table 2).
35 However, given the fact that **TPD** is a weaker acceptor than **BT**,
the absorption spectra of **Si4T-TPD** were significantly blue

shifted, both in solution and thin film and the bandgap was raised
by 0.1 eV. In thin film, the absorption band of **Si4T-TPD**
presents a more defined vibronic structure, than in solution, with
two peak maxima at 615 nm and at 668 nm, respectively. In order
45 to reduce the HOMO energy level of the **Si4T** polymers without
compromising the bandgap, monomer **7** was co-polymerized with
5,6-difluorobenzo[*c*][1,2,5]thiadiazole (**2FBT**). Due to the
electron withdrawing character of fluorine, both frontier energy
levels should be similarly lowered and therefore the bandgap is
50 expected to remain unaffected.[12] The absorption spectrum of
Si4T-2FBT in solution is nearly identical to that of **Si4T-BT**. In
the solid state, however there are significant differences between
the spectra of both polymers. The **Si4T-2FBT** spectrum is further
red-shifted than the **Si4T-BT** spectrum, perhaps correlated to the
55 higher number average molecular weight of **Si4T-2FBT**. The
Si4T-BT absorption band shows some indication of a shoulder at
lower wavelengths, whereas the absorption band of **Si4T-2FBT**
presents a well defined shoulder feature at higher energies. We
speculate that the more defined vibronic structure of the **Si4T-**
60 **2FBT** absorption band is caused by a reduction of the rotational
freedom between donor and acceptor units in the polymer
backbone, due to favourable attractive interactions between the
sulphur's lone pair electrons on the **Si4T** unit and the
electronegative fluorine atoms on the adjacent **BT** moiety. This
65 hypothesis is also supported by the quantum mechanical
calculations, which suggest a dihedral angle of 3.87° between the
Si4T and the **BT** unit and a slightly smaller angle of 2.87° in case
of the **Si4T-2FBT** polymer. The barrier of planarization, defined
as the difference between the energy of the planar (constraint)
70 and the fully optimized structures, of **Si4T-BT** amounts to 0.23

Table 1. Molecular Weights and Thermal Stability of the **Si4T** Polymers

Polymer	$M_n{}^a$ (kg/mol)	$M_w{}^b$ (kg/mol)	PDI^c	$T_d{}^d$ (°C)
Si4T-BT	19	53	2.8	428
Si4T-TPD	21	26	1.2	423
Si4T-2FBT	40	58	1.5	428

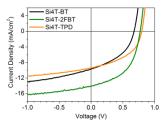*a* Number-average molecular weight. *b* Weight-average molecular weight.
c M_w/M_n. *d* Decomposition temperature (5% weight loss) determined by
40 thermal gravimetric analysis under nitrogen.

Table 2. Optical Properties and Frontier Energy Levels of **Si4T** Polymers

Polymer	$\lambda_{max}{}^a$ (nm)	$\lambda_{max}{}^b$ (nm)	exp. HOMO / LUMO^c (eV)	calc. HOMO / LUMO^d (eV)	$E_g{}^e$
Si4T-BT	694	714	-5.0 / -3.4	-4.5 / -3.1	1.6
Si4T-TPD	651	668	-5.3 / -3.6	-4.7 / -2.9	1.7
Si4T-2FBT	684	731	-5.1 / -3.5	-4.6 / -3.1	1.6

a Dilute CB solution. *b* Thin film spin-coated from CB solution (5 mg/ml,
1000 rpm). *c* LUMO energy level estimated by adding the absorption
onset to the HOMO energy level which was measured by photoelectron
75 spectroscopy in air. *d* energy levels calculated by DFT using B3LYP/6-
31G* model. *e* Optical band gap determined from the onset of absorption
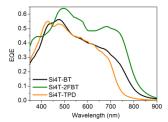in the solid state.

Figure 2. J-V curve (left) and external quantum efficiencies spectra (right) of **Si4T**-polymer:PC$_{71}$BM OPV devices.

kJ/mol, which is nearly double the energy needed to planarize **Si4T-2FBT** (0.12 kJ/mol).

The HOMO energy levels of **Si4T-BT** and **Si4T-2FBT** are both higher than the corresponding silaindacenodithiophene (**SiIDT**) polymers previously reported.[13, 14] The increase in HOMO energy level confirms that the incorporation of the more electron rich thieno[3,2-*b*]thiophene into the **IDT** unit significantly increases the electron rich character of the fused ring system. The absorption spectra of **Si4T** polymers are about 60-80 nm red shifted compared to **SiIDT** polymers. When blended with [6,6]-phenyl C71 butyric acid methyl ester (PC$_{71}$BM), **Si4T-BT** afforded a V_{OC} of 0.67 V and a short-circuit current (J_{SC}) of 9.67 mA/cm^2 in OPV devices, which corresponds to a rather low photocurrent efficiency (PCE) of 2.79% (Table 3). The **Si4T-TPD** polymer has a much lower HOMO energy level, which translates into a higher V_{OC} of 0.80 V (Figure 3). However, a similar J_{SC} value of 9.42 mA/cm^2 and the moderate FF of 0.46 resulted in average device performances of 3.46%. The **Si4T-2FBT** polymer exhibited the best performance in OPV devices. The low HOMO energy level of the **Si4T-2FBT** polymer manifests as a large V_{OC} of 0.77 V comparable to the **Si4T-TPD** polymer, but the J_{SC} increased by nearly 70% to 14.07 mA/cm^2 which led to high device efficiencies of 5.52%. The external quantum efficiency (EQE) spectra are shown in Figure 2 and all three devices exhibit a broad response from 350 up to 750 nm for **Si4T-TPD**, up to 800 nm in the cases of **Si4T-BT** and **Si4T-2FBT,** respectively. However, the lower EQE response at higher wavelengths suggests that in the case of **Si4T-BT** and **Si4T-TPD** most of the current is generated by the PC$_{71}$BM and not by polymer excitons. **Si4T-2FBT** is the only of the three polymers with an EQE above 40% between 600 and 750 nm, which therefore contributes significantly to the charge generation in the OPV device at higher wavelengths.

The surface morphologies of the polymer:PC$_{71}$BM blends were studied by atomic force microscopy (Figures S10 to S12 in the ESI). All blends form very smooth high quality films when spin-casted from *o*-dichlorobenzene. The three films are very homogenous with little apparent phase separation and low surface roughness. The **Si4T-2FBT** film is slightly rougher than the other

Table 3. Photovoltaic Properties of the **Si4T** Polymers

Polymer	J_{SC} (mA/cm^2)	V_{OC} (V)	FF	PCE (%)
Si4T-BT	9.69	0.67	0.43	2.79
Si4T-TPD	9.42	0.80	0.46	3.46
Si4T-2FBT	14.07	0.77	0.51	5.52

Conventional device architecture ITO/PEDOT:PSS/polymer:PC$_{71}$BM/ Ca/Al with a polymer:PC$_{71}$BM blend ratio of 1:3.5 processed from *o*-dichlorobenzene.

films and contains small granular features. The formation of these granular domains might be favoured by the higher molecular weight component of the polymer, which tends to preferentially favour phase separation from the PC$_{71}$BM.

In conclusion, we have synthesized a novel thieno[3,2-*b*]thiophene based ladder type donor monomer, whose fused and planar structure was determined by single crystal X-ray diffraction. The incorporation of silicon bridging atoms allowed the introduction of linear alkyl side chains onto the novel thieno[3,2-*b*]thienobis(silolothiophene) monomer and we synthesized three soluble and easily processable new donor-acceptor polymers. By judiciously choosing the acceptor monomer, we were able to adjust the polymer frontier energy levels, which lead to high V_{OC} values and excellent PCE values of 5.52% in OPV devices.

Notes and references

^{a} Department of Chemistry and Centre for Plastic Electronics, Imperial College London, London, SW7 2AZ, UK; E-mail: r.ashraf@imperial.ac.uk

^{b} Department of Physics and Centre for Plastic Electronics, Imperial College London, London, SW7 2AZ, UK

^{c} CSIRO Materials Science and Engineering, VIC 3169, Australia

1. G. Dennler, M. C. Scharber, T. Ameri, P. Denk, K. Forberich, C. Waldauf and C. J. Brabec, *Advanced Materials*, 2008, **20**, 579-583.

2. J. Peet, A. J. Heeger and G. C. Bazan, *Accounts of Chemical Research*, 2009, **42**, 1700-1708.

3. C. L. Chochos and S. A. Choulis, *Progress in Polymer Science*, 2011, **36**, 1326-1414.

4. C. Yu, L. Chen, S. Chan, G. Hwang, C. Ting, *Chemistry of Materials*, 2009, **21**, 3262-3269.

5. W. M. Zhang, J. Smith, S. E. Watkins, R. Gysel, M. McGehee, A. Salleo, J. Kirkpatrick, S. Ashraf, T. Anthopoulos, M. Heeney and I. McCulloch, *Journal of the American Chemical Society*, 2010, **132**, 11437-11439.

6. H. Bronstein, D. S. Leem, R. Hamilton, P. Woebkenberg, S. King, W. M. Zhang, R. S. Ashraf, M. Heeney, T. D. Anthopoulos, J. de Mello and I. McCulloch, *Macromolecules*, 2011, **44**, 6649-6652.

7. J. Wang, S. K. Hau, H. Yip, J. A. Davies, K. Chen, Y. Zhang, Y. Sun and A. K.-Y. Jen, *Chemistry of Materials*, 2011, **23**, 765-767.

8. I. McCulloch, R. S. Ashraf, L. Biniek, H. Bronstein, C. Combe, J. E. Donaghey, D. I. James, C. B. Nielsen, B. C. Schroeder and W. Zhang, *Accounts of Chemical Research*, 2012, **45**, 714-722.

9. J. Ohshita, *Macromolecular Chemistry and Physics*, 2009, **210**, 1360-1370.

10. H. Bronstein, R. S. Ashraf, Y. J. Kim, A. J. P. White, T. Anthopoulos, K. Song, D. James, W. M. Zhang and I. McCulloch, *Macromolecular Rapid Communications*, 2011, **32**, 1664-1668.

11. Y.-J. Cheng, C.-H. Chen, T.-Y. Lin and C.-S. Hsu, *Chemistry – An Asian Journal*, 2012, **7**, 818-825.

12. H. Zhou, L. Yang, A. C. Stuart, S. C. Price, S. Liu and W. You, *Angewandte Chemie International Edition*, 2011, **50**, 2995-2998.

13. R. S. Ashraf, Z. Y. Chen, D. S. Leem, H. Bronstein, W. M. Zhang, B. Schroeder, Y. Geerts, J. Smith, S. Watkins, T. D. Anthopoulos, H. Sirringhaus, J. C. de Mello, M. Heeney and I. McCulloch, *Chemistry of Materials*, 2011, **23**, 768-770.

14. B. C. Schroeder, Z. Huang, R. S. Ashraf, J. Smith, P. D'Angelo, S. E. Watkins, T. D. Anthopoulos, J. R. Durrant and I. McCulloch, *Advanced Functional Materials*, 2012, **22**, 1663-1670.